J. Fluid Mech. (1965), *vol.* 22, *part* 2, *pp.* 257–271
Printed in Great Britain

The decay of a turbulent swirl in a pipe

By FRANK KREITH AND O. K. SONJU
University of Colorado, Boulder, Colorado

(Received 16 April 1964 and in revised form 22 January 1965)

This paper presents a linearized theory for the average decay of a tape-induced fully developed turbulent swirl in flow through a pipe. In the Reynolds number range between 10^4 and 10^5 the theoretical analysis was found to be in good agreement with experimental data obtained with water in a 1 in. pipe, provided the eddy diffusivity was chosen appropriately.

It was observed that a turbulent swirl decays to about 10–20 % of its initial intensity in a distance of about 50 pipe diameters, the decay being more rapid at smaller than at larger Reynolds numbers. The theoretical swirl velocity distribution agreed qualitatively with experimental measurements at distances less than 20 diameters downstream from the outlet of the swirl inducer, but deviated from the experimental results further downstream.

1. Introduction

Problems related to the dynamics of turbulent vortical flow systems have recently received considerable attention. Reynolds (1961*a*, *b*), Deissler & Perlmutter (1960), and Sibulkin (1962)† have treated a variety of vortical flow problems in order to explain and analyse the phenomena taking place in a vortex tube. Kerrebrock & Meghreblian (1961), Keyes (1960) and Ragsdale (1961) have studied other types of vortex flows in an effort to develop a method suitable for the containment of gases in a fission rocket. Kreith & Margolis (1959), Smithberg & Landis (1964), and Gambill, Bundy & Wansbrough (1961) studied forced turbulent swirl flows in tubes with tape inserts with a view towards improving heat exchanger performance. This paper presents the results of an experimental and analytical study of the decay of an incompressible, tape-induced turbulent swirl in a tube. The results of this study may have applications in technical devices such as a heat exchanger or a nuclear rocket, but no attempt will be made here to relate this work to any particular device.

2. The governing equations

From the continuity and Navier–Stokes equations in the co-ordinates and notation indicated in figure 1, on taking mean values with respect to time and requiring the mean motion to be steady, incompressible, and axisymmetric (Hinze 1959), the following system of equations are obtained:

$$\frac{\partial U}{\partial x}+\frac{1}{r}\frac{\partial (rV)}{\partial r}=0, \tag{1}$$

† This reference contains a complete summary of the work prior to 1960.

$$U\frac{\partial U}{\partial x}+V\frac{\partial U}{\partial r}=-\frac{1}{\rho}\frac{\partial P}{\partial x}+\nu\left[\frac{\partial^2 U}{\partial x^2}+\frac{\partial^2 U}{\partial r^2}+\frac{1}{r}\frac{\partial U}{\partial r}\right]-\left[\frac{\partial}{\partial x}\overline{u^2}+\frac{1}{r}\frac{\partial}{\partial r}r\,\overline{uv}\right], \tag{2}$$

$$U\frac{\partial V}{\partial x}+V\frac{\partial V}{\partial r}-\frac{W^2}{r}=-\frac{1}{\rho}\frac{\partial P}{\partial r}+\nu\left[\frac{\partial^2 V}{\partial x^2}+\frac{\partial^2 V}{\partial r^2}+\frac{1}{r}\frac{\partial V}{\partial r}-\frac{V}{r^2}\right]-\left[\frac{\partial}{\partial x}\overline{uv}+\frac{1}{r}\frac{\partial}{\partial r}r\,\overline{v^2}-\frac{\overline{w^2}}{r}\right], \tag{3}$$

$$U\frac{\partial W}{\partial x}+V\frac{\partial W}{\partial r}+\frac{VW}{r}=\nu\left[\frac{\partial^2 W}{\partial x^2}+\frac{\partial^2 W}{\partial r^2}+\frac{1}{r}\frac{\partial W}{\partial r}-\frac{W}{r^2}\right]-\left[\frac{\partial}{\partial x}\overline{uw}+\frac{\partial}{\partial r}\overline{vw}+2\frac{\overline{vw}}{r}\right]. \tag{4a}$$

These equations are non-linear, there are more dependent variables than governing equations, and no general method of solution exists. In the absence of general principles on which further mathematical relationships might be based, we are forced to seek an approximate solution by simplifying the equations with the aid of an order of magnitude analysis.

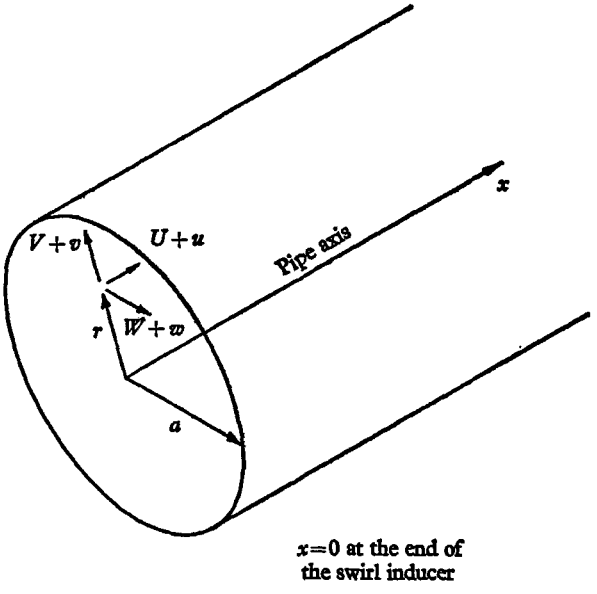

FIGURE 1. Co-ordinate system and velocity notation.

3. Solution of the swirl equation

Experiments in turbulent as well as laminar flow (Smithberg & Landis 1964; Talbot 1954) have shown that as a result of the swirl the axial velocity decreases near the centre of the pipe and increases near the wall. This is illustrated by the data of Smithberg & Landis shown in figure 2 in dimensionless form. Since these data were obtained with twisted metal tapes, identical to those used in the experimental phase of this study, they can be used directly to establish an average initial velocity profile.

Substituting U_1+u' for U in (4), which will be called the swirl equation, yields terms of the form $U_1\dfrac{\partial W}{\partial x}$ and $u'\dfrac{\partial W}{\partial x}$, where U_1 is the mean axial velocity profile in fully-developed axial pipe flow. An order of magnitude analysis shows that the latter terms are negligible compared to the former.

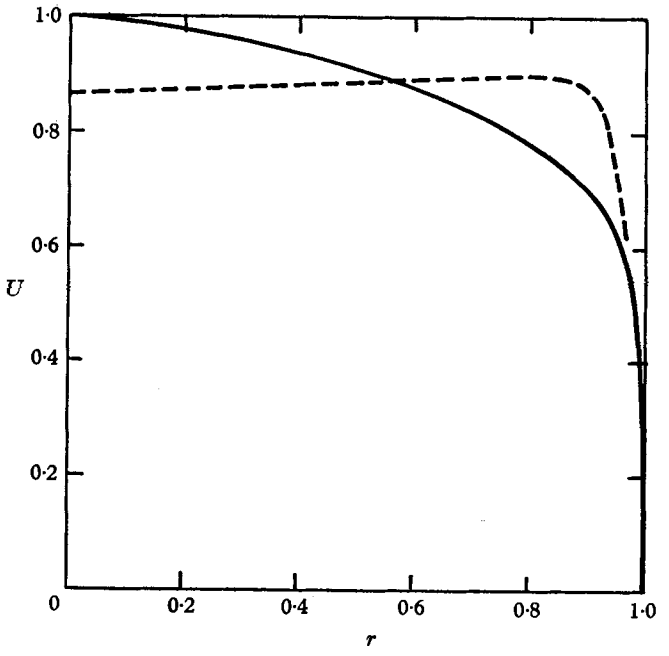

FIGURE 2. Mean axial velocity distribution according to Laufer (1954) (——, $U_1 = U(r, \infty)$) and Smithberg & Landis (1964), $H = 20$ (– –, $U(r, 0)$).

The boundary conditions which must be satisfied are

$$V = W = 0, \quad \frac{\partial U}{\partial r} = 0 \quad \text{at} \quad r = 0,$$

$$U = V = W = 0 \quad \text{at} \quad r = a,$$

where a is the tube radius. Using the boundary condition for V and noting that $\partial U/\partial x$ is very small, (1) shows that V is also small so that the term

$$V(\partial W/\partial r + W/r)$$

can be neglected in (4a). An analysis of the results obtained in a decaying laminar swirl (Talbot 1954) suggests that in turbulent flow the term $\nu(\partial^2 W/\partial x^2)$ will be negligible compared to $U(\partial W/\partial x)$. Using data for fully-developed turbulent flow in a pipe (Laufer 1954) as a guide for the phenomena occurring in the present problem, it seems reasonable to expect that on the average also the term $\partial\overline{wu}/\partial x$ is an order of magnitude smaller than the term $U\,(\partial W/\partial x)$.

In a number of vortex flow systems it has been shown (Gambill *et al.* 1961; Keyes, 1960; Ragsdale 1961; Reynolds 1961a) that the Reynolds stress $\rho\overline{vw}$ can be approximated by $-\epsilon(\partial W/\partial r - W/r)$ where ϵ is the so-called eddy diffusivity. In general ϵ is a variable in a flow system, but experiments have shown (Deissler & Perlmutter 1960; Keyes 1960; Einstein & Li 1951) that it does not vary appreciably with r in a vortex. Although this experimental evidence was gathered in systems having geometrical configurations different from the one treated here, if one assumes that the basic structure of the $\rho\overline{vw}$ term does not change from one vortex system to another, the available data can be applied to the problem at

hand. Moreover, because of the predominance of the axial velocity in the case treated here (Musolf 1963), the value of ϵ will also be assumed independent of x.

With the simplifications outlined above, the swirl equation reduces to the form

$$U_1 \frac{\partial W}{\partial x} = (\nu + \epsilon)\left(\frac{\partial^2 W}{\partial r^2} + \frac{1}{r}\frac{\partial W}{\partial r} - \frac{W}{r^2}\right). \tag{4b}$$

This equation is linear and a solution by the method of separation of variables is feasible. However, before carrying out the detailed steps of this solution, it will be convenient to non-dimensionalize the equation by expressing the velocities, the distances and the eddy diffusivity as fractions of U_0, a and ν respectively. U_0 is the maximum value of U_1.

Equation (4b) then takes the form

$$\frac{\partial^2 W}{\partial^2 r} + \frac{1}{r}\frac{\partial W}{\partial r} - \frac{W}{r^2} = \frac{N_R}{1+\epsilon} U_1 \frac{\partial W}{\partial x}, \tag{4c}$$

where N_R is the axial flow Reynolds number $U_0 a/\nu$.

Assuming a solution of the form

$$W(r, x) = R(r)\, X(x)$$

and substituting this expression into (4c), one obtains after rearranging

$$\frac{d^2 R_n(r)/dr^2 + r^{-1} dR_n(r)/dr - r^{-2} R_n(r)}{U_1 R_n(r)} = \frac{N_R}{1+\epsilon}\frac{dX_n(x)/dx}{X_n(x)} = -\lambda_n^2, \tag{5}$$

where λ_n^2 are the eigenvalues and $R_n(r)$ are the eigenfunctions. The eigenvalues are taken as positive and the minus sign must therefore be used in order to satisfy the physical problem.

The right-hand side of (5) implies that

$$\frac{dX_n}{dx} + \frac{\lambda_n^2(1+\epsilon)}{N_R} X_n = 0, \tag{6a}$$

with solution

$$X_n(x) = A_n \exp\left[-\frac{\lambda_n^2(1+\epsilon)}{N_R} x\right], \tag{6b}$$

where A_n is an arbitrary constant.

The r-dependent part of (5) is

$$\frac{d^2 R_n}{dr^2} + \frac{1}{r}\frac{dR_n}{dr} + \left(\lambda_n^2 U_1 - \frac{1}{r^2}\right) R_n = 0, \tag{7a}$$

and the transformed boundary conditions are $R_n(0) = R_n(1) = 0$.

If U_1 is taken as a constant in (7a), the solution can be expressed in terms of first-order Bessel functions. A better approximation can be obtained by using Laufer's data for flow in a pipe (1954), which indicate that $U_1 = (1-r)^{\frac{1}{7}}$ with good accuracy in the Reynolds number range from 10^4 to 10^5. Using this variation in U_1 as a perturbation term, (7) can be solved, as shown by Courant & Hilbert (1953), by a method of approximations.

The perturbed differential equation can be written in the form

$$LR_n - \alpha \lambda_n^2 (1 - U_1) R_n + \lambda_n^2 R_n = 0, \tag{7b}$$

where the operator

$$L = d^2/dr^2 + r^{-1}\,d/dr - r^{-2}$$

and α is a perturbation parameter in terms of which the solution will be expanded. In the present case α will be set equal to 1·0 in order to satisfy (7*a*).

Neglecting first the perturbed term in (7*b*), the solution is $\bar{R}_n = B_n J_1(\bar{\lambda}_n r)$, where $\bar{R}_n$ and $\bar{\lambda}_n^2$ denote the appropriate eigenfunctions and eigenvalues, $J_1(\bar{\lambda}_n r)$ is the Bessel function of the first kind of order one, and B_n is an arbitrary constant. Since the perturbation theory assumes the boundary conditions on the perturbed and unperturbed eigenfunctions to be identical, one has

$$\bar{R}_n(0) = 0 \quad \text{and} \quad \bar{R}_n(1) = 0.$$

The first boundary condition $\bar{R}_n(0) = 0$ is satisfied since $J_1(\bar{\lambda}_n 0) = 0$. The second boundary condition, $\bar{R}_n(1) = 0$, requires that $J_1(\bar{\lambda}_n 1) = 0$. The zeros of $J_p(x_n)$ are well known, and for $p = 1$ Jahnke & Emde (1945) list them as

$$\bar{\lambda}_1^2 = 14{\cdot}684, \quad \bar{\lambda}_2^2 = 49{\cdot}224, \quad \bar{\lambda}_3^2 = 103{\cdot}490, \quad \bar{\lambda}_4^2 = 177{\cdot}529\ldots. \tag{8}$$

The next assumption made in the perturbation theory is that the eigenfunctions, as well as the eigenvalues, may be expanded in powers of α, or

$$R_n(r) = \bar{R}_n + \alpha p_n + \alpha^2 q_n + \ldots, \tag{9}$$

$$\lambda_n^2 = \bar{\lambda}_n^2 + \alpha\beta_n + \alpha^2\gamma_n + \ldots, \tag{10}$$

where the eigenfunctions $R_n(r)$ and $\bar{R}_n(r)$ are normalized.

Substituting these expressions into (7*b*) and evaluating the two first approximations yields

$$\left.\begin{aligned} R_1(r) &\approx (2/J_0^2(\bar{\lambda}_1))^{\frac{1}{2}} J_1(\bar{\lambda}_1 r) = 3{\cdot}51\,J_1(\bar{\lambda}_1 r), \\ R_2(r) &\approx (2/J_0^2(\bar{\lambda}_2))^{\frac{1}{2}} J_1(\bar{\lambda}_2 r) = 4{\cdot}72\,J_1(\bar{\lambda}_2 r), \\ R_3(r) &\approx (2/J_0^2(\bar{\lambda}_3))^{\frac{1}{2}} J_1(\bar{\lambda}_3 r) = 5{\cdot}66\,J_1(\bar{\lambda}_3 r), \\ R_4(r) &\approx (2/J_0^2(\bar{\lambda}_4))^{\frac{1}{2}} J_1(\bar{\lambda}_4 r) = 6{\cdot}47\,J_1(\bar{\lambda}_4 r), \ \ldots \end{aligned}\right\} \tag{11}$$

and $$\lambda_1^2 \approx 16{\cdot}68, \quad \lambda_2^2 \approx 55{\cdot}71, \quad \lambda_3^2 \approx 117{\cdot}86, \quad \lambda_4^2 \approx 203{\cdot}73, \ldots. \tag{12}$$

The details of this solution are shown in the Appendix.

The initial condition on $W(r, x)$ is $W(r, 0) = f(r)$. To satisfy this initial condition a series solution of the form

$$W(r, x) = \sum_{n=1}^{\infty} C_n J_1(\bar{\lambda}_n r) \exp\left[-\frac{\lambda_n^2(1+\epsilon)}{N_R} x\right] \tag{13}$$

is assumed, and one has

$$W(r, 0) = f(r) = \sum_{n=1}^{\infty} C_n J_1(\bar{\lambda}_n r).$$

Since the first-order Bessel functions are orthogonal with respect to the weight function r, C_n can be expressed as

$$C_n = \frac{\int_0^1 r f(r) J_1(\bar{\lambda}_n r)\,dr}{\int_0^1 r J_1^2(\bar{\lambda}_n r)\,dr} = \frac{2}{J_0^2(\bar{\lambda}_n)} \int_0^1 r f(r) J_1(\bar{\lambda}_n r)\,dr. \tag{14}$$

The theoretical determination of $W(r, x)$ is now complete, and may be used to check the experimental data as soon as the initial condition and the eddy diffusivity of the flow in the system are known.

4. The initial condition

In order to derive a theory for the flow and heat transfer in tubes with swirling flow, Smithberg & Landis (1964) made velocity measurements at the outlet section of a 1·328 in. diameter tube with twisted tape inserts having pitches from 3·6 to 22·0 pipe diameters. The pitch is defined as the axial distance for a 360-degree twist of the tape. They obtained velocity profiles in the Reynolds number range of interest here and these measurements were used to establish the initial condition for the problem at hand because the experimental velocity profiles obtained in the present work were only of a qualitative nature. The initial swirl velocity profile is shown in figure 3 in dimensionless form. The measurements of Smithberg & Landis indicate that the swirl velocity and the axial velocity profiles are not completely axisymmetric because of secondary flows created in the swirl inducer section. Since the theory assumes axisymmetric flow, an average profile was used as shown in figure 3, where also the magnitude of the deviations from this average profile due to secondary flows are indicated.

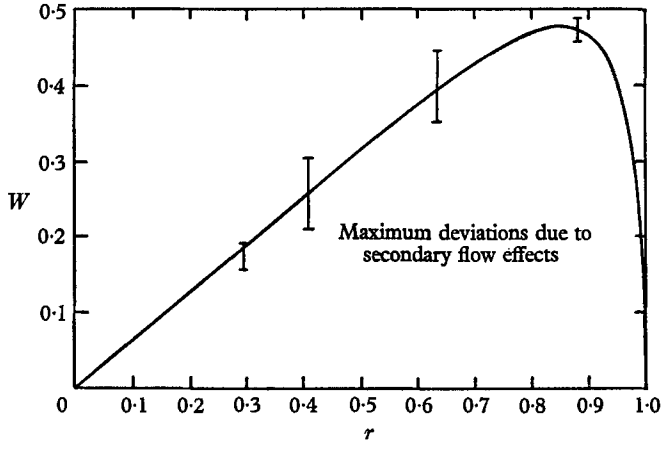

FIGURE 3. Initial swirl velocity distribution for $H = 10$ according to Smithberg & Landis (1964).

The initial condition shown in figure 3 can be approximated by the expression

$$W(r, 0) = f(r) = H^{-1}[6{\cdot}3r - 0{\cdot}013(1{\cdot}1 - r)^{-2{\cdot}68}],$$

which has a maximum of 0·48 at $r \simeq 0{\cdot}85$ when H, the non-dimensional pitch of the inducer tape, has a value of 10.

The coefficients C_n, found by numerical integration of (14), are

$$C_1 = 7{\cdot}78/H,\ C_2 = -5{\cdot}26/H,\ C_3 = 3{\cdot}93/H,\ C_4 = -3{\cdot}16/H. \qquad (15)$$

From (13) the swirl velocity distribution can then be written as

$$W(r,x)=\frac{7\cdot78}{H}J_1(3\cdot832r)\exp\left[-\frac{16\cdot7(1+\epsilon)x}{N_R}\right]-\frac{5\cdot26}{H}J_1(7\cdot016r)\exp\left[-\frac{55\cdot7(1+\epsilon)x}{N_R}\right]$$
$$+\frac{3\cdot93}{H}J_1(10\cdot174r)\exp\left[-\frac{117\cdot9(1+\epsilon)x}{N_R}\right]$$
$$-\frac{3\cdot16}{H}J_1(13\cdot324r)\exp\left[-\frac{203\cdot7(1+\epsilon)x}{N_R}\right]+\ldots. \quad (16)$$

5. The eddy diffusivity for the Reynolds stress term $\rho\overline{vw}$

The swirl velocity $W(r,x)$ for the tape-induced swirl can be determined from (16) provided ϵ, the dimensionless value of the eddy diffusivity, can be ascertained in some way. Fortunately, the eddy diffusivity in a vortex flow has been measured independently by Ragsdale (1961) as well as by Keyes (1960) and their results can be modified to satisfy the problem at hand as shown below. In these investigations, the swirl was induced by tangential jets along the periphery of the tube and the axial flow was very small compared to the swirl. The experimental set-ups differed principally in the aspect ratio of the test section, which was 6 in Keyes's work, but less than one in Ragsdale's. The data of these two studies are plotted in figure 4 of Ragsdale (1961).

Keyes correlated his data, which extended over a range of tangential Reynolds numbers from 4×10^4 to 1×10^6, by the method of least squares and proposed the equation $\epsilon=2\cdot03\times10^{-3}(N_{R,t})^{0\cdot86}$. The Reynolds number exponent in this correlation is in close agreement with results of the Martinelli (1947) analogy for turbulent flow in a pipe which predicts an exponent of 0·90 for the variation of ϵ with axial-flow Reynolds number. Ragsdale obtained data only over a very small range of Reynolds numbers (5×10^5 to 1×10^6); by means of a heuristic similarity argument he suggested that ϵ should be directly proportional to the Reynolds number and his correlation line fits the equation $\epsilon=1\cdot4\times10^{-3}N_{R,t}$. In the Reynolds number range for which both Keyes and Ragsdale obtained data, the values of eddy diffusivity measured by the latter are considerably larger.

In view of the fact that in the present study the axial flow was substantial, it seemed more appropriate to use the exponent of 0·86, which is in substantial agreement with pure axial flow results of Martinelli. But in view of the disagreement in the measured magnitude of ϵ it was decided to perform an experiment to select a value of ϵ which would fit the present situations at one axial Reynolds number and then use Keyes's functional relationship to extend the measured value to other conditions.

The swirl decay was measured at an axial flow Reynolds number of 61,000 and the value of ϵ which correlated the decay characteristics predicted by theory and those which were observed experimentally was calculated and found, within the accuracy of the experimental data, independent of the swirl intensity, to be 54. This value, in conjunction with the appropriate exponent, yielded the correlation equation

$$\epsilon=4\cdot15\times10^{-3}N_R^{0\cdot86}, \quad (17)$$

where, in view of the predominance of the axial velocity component, an average

for all pitches was used to make the swirl decay independent of the initial swirl intensity.

The foregoing method of evaluating ϵ is clearly empirical. However, having once established at one Reynolds number the appropriate scaling factor for Keyes's data, the eddy diffusivity calculated by this technique combined with the analysis presented in the preceding section yielded good agreement between experimental results and theoretical predictions for average swirl decays at other Reynolds numbers, as will be shown below. It would undoubtedly be more satisfactory if one could predict the eddy diffusivity from more fundamental principles, but at the present state of our understanding of turbulent transport phenomena recourse to at least one empirical step seems to be unavoidable. At the same time, however, it is to be hoped that experience with successful guesses or empirical approaches, as were used in this study, will eventually point the way towards general and more basic principles.

6. Experimental measurements

In order to verify the theoretical analysis of the swirl decay in a pipe, a series of experiments were performed in which the decay of a swirl induced into the flow through a 1 in. pipe by means of twisted tape swirl inducers was measured over a range of axial Reynolds numbers from 10^4 to about 10^5. The general arrangement of the equipment is shown schematically in figure 4 and a photograph of

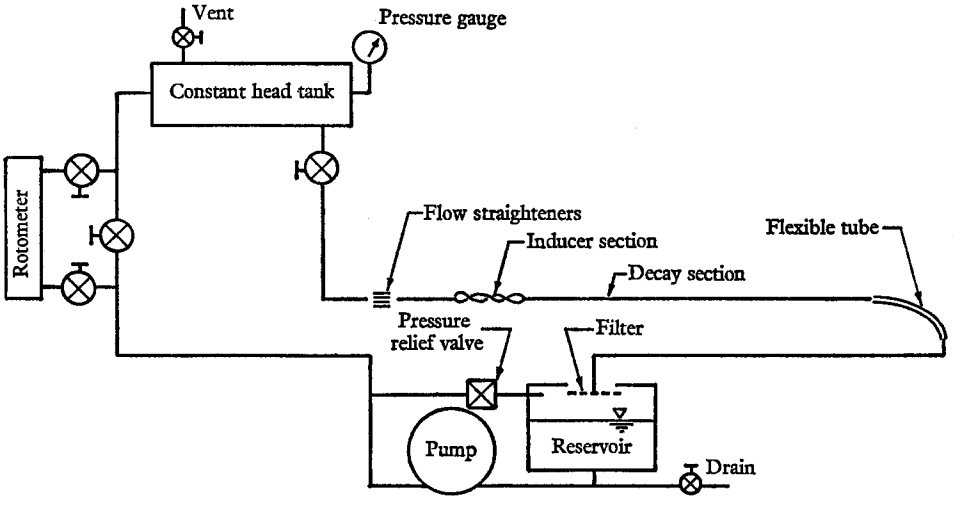

FIGURE 4. Schematic sketch of experimental equipment.

the test set-up is presented in figure 5 (plate 1). Water from a constant head tank entered the test section, which consisted of a 1 in. I.D. plastic tube, about 100 in. long. A swirl was introduced into the flow by means of a twisted tape inducer inserted in the inlet section as shown in figure 6 (plate 2). The twisted tape inducers used in the experiments consisted of 0·0336 in. thick galvanized steel strips and were similar in construction to those used previously by Kreith & Margolis (1959), Gambill *et al.* (1961), and Smithberg & Landis (1964).

Two different types of swirl inducers were used in the experiments. One had a dimensionless pitch H of 9 which was about the tightest obtainable without buckling the tape. The other inducer had a pitch of 15. Both inducers were sufficiently long to obtain a fully-developed swirl velocity profile at the outlet of the inducer section.

The average swirl in the pipe was measured at various distances downstream from the outlet of the inducer section by means of a swirl vortex meter shown in figure 6. This meter consisted of a flat blade, which was free to rotate about an axial shaft in the centre of the tube. The blade extended 0·437 in. radially from the centre line of the pipe in both directions and was 0·25 in. long in the axial direction; its rotational speed was measured by means of a stroboscope.

The measured angular velocities of the blade are plotted as a function of distance from the inducer outlet in figures 7 and 8 for both inducer tapes; the data shown were obtained at Reynolds numbers of 61,000 and 18,000 respectively. In both figures the data are presented in percentage of the initial swirl *vs* the dimensionless axial distance x. The experiments indicate that the rate of decay depends on the axial Reynolds number: the decay rate increases as the Reynolds number decreases, but within the experimental accuracy the decay was found to be independent of H or, equivalently, of the initial swirl intensity.

The swirl decay measurements obtained in this study do not yield velocity profiles since the radial velocity of the swirl meter is only representative of an 'average' angular rotation of the fluid in the pipe. The experimental measurements can, however, be compared with the theoretically predicted decay characteristics in the following manner. Neglecting the friction of the bearing in the swirl meter, the expected angular velocity of rotation of the meter blade ω_A can be calculated from the moment of momentum about the axis of the swirl over the area of the blade, or

$$\frac{\omega_A}{U_0/a} = \frac{2}{r_B^2}\left[\int_0^{r_B} W^2 r\,dr\right]^{\frac{1}{2}}, \tag{18}$$

where r_B is the radial length of the blade.

Combining (18) with (16) gives an expression which can be evaluated with satisfactory accuracy with the first three terms in the series

$$\frac{\omega_A}{U_0/a} \simeq \frac{2{\cdot}615}{H}\left\{4{\cdot}84\exp\left[-\frac{33{\cdot}4(1+\epsilon)x}{N_R}\right] + 1{\cdot}18\exp\left[-\frac{111{\cdot}4(1+\epsilon)x}{N_R}\right] - 0{\cdot}152\exp\left[-\frac{72{\cdot}4(1+\epsilon)x}{N_R}\right] + \ldots\right\}^{\frac{1}{2}}, \tag{19}$$

for values of x more than one or two diameters downstream from the outlet of the inducer section, and, from the initial velocity profile given in § 4, one obtains $\omega_A/(U_0/a) = 6{\cdot}0/H$.

The results of the theoretical analysis and the experiments are compared in figures 7 and 8. An inspection of these figures shows that the measured 'average' swirl decay characteristics are in very good agreement with the theoretically predicted swirl decay.

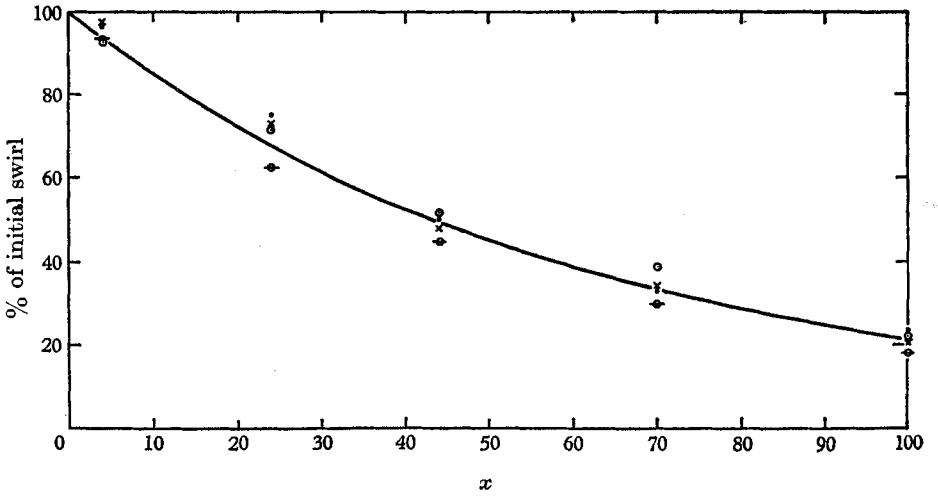

FIGURE 7. Comparison of experimentally measured and theoretically predicted swirl decay at a Reynolds number of 61,000. Experimental data in 1 in. pipe for various inducers. •, Pitch 15, length 30 in.; ×, pitch 9, length 30 in.; ⊙, pitch 9, length 18 in.; ⊖, pitch 15, length 18 in.; ———, theory.

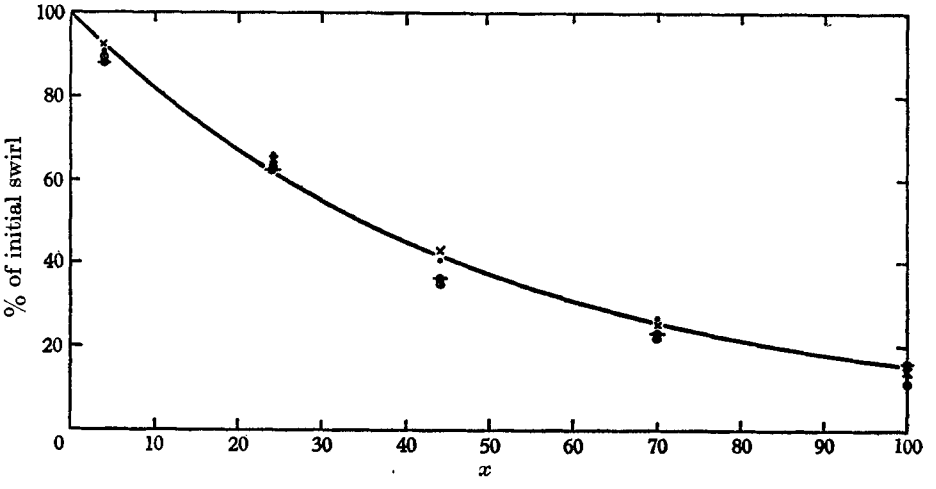

FIGURE 8. Comparison of experimentally measured and theoretically predicted swirl decay at a Reynolds number of 18,000. Experimental data in 1 in. pipe for various inducers. •, Pitch 15, length 30 in.; ×, pitch 9, length 30 in.; ⊙, pitch 9, length 18 in.; ⊖, pitch 15, length 18 in.; ——, theory.

The analysis predicts not only the swirl decay, but also the velocity distribution downstream from the inducer section. An attempt was, therefore, made to compare the theoretically predicted velocity distribution with some measurements made in a 2 in. I.D. tube by Musolf (1963) in a geometrically similar system with a directional Pitot tube. These experimental data are qualitative rather than quantitative because the axial and tangential velocity components were not measured directly, but were calculated from measurements of the local flow

direction and the mass rate of flow through the pipe, using an axial velocity distribution approximated from figure 2 and the relation

$$W(r,x) = U(r,x)\tan\beta, \tag{20}$$

where β is the angle between the axis of the pipe and the direction of the net velocity vector.

Some of the results are shown in figure 9. Comparing these profiles with the theoretical swirl velocity distribution shows general agreement near the swirl inducer, i.e. within a distance less than about 20 diameters downstream from the outlet of the inducer section. Further downstream, where the theory predicts profiles with a radial distribution proportional to $J_1(3{\cdot}83r)$, the experimental

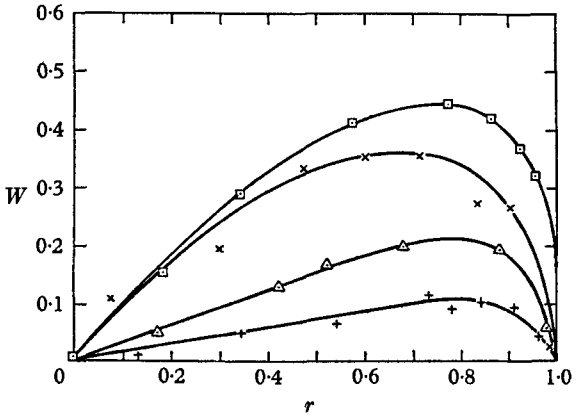

FIGURE 9. Experimentally measured tangential velocity profiles at a Reynolds number of 48,000. Tangential velocity: ⊡, $x = 6$; ×, $x = 10$; △, $x = 47$; +, $x = 100$. Axial velocity, 6·24 ft./sec. Reynolds number, 48,000; inducer pitch, 10.

profiles are more triangular in shape with a maximum velocity at a radial distance from the centre line of about 0·80 % of the pipe radius. In passing, it should be noted that the integral equation (Sonju 1962)

$$\frac{d}{dx}\int_0^1 \left(UW + \frac{\overline{uw}}{U_0^2}\right) r^2 dr = \frac{1}{N_R}\left(\frac{\partial W}{\partial r}\right)_{r=1}$$

was used to estimate $(\partial W/\partial r)_{r=1}$ and, although owing to a lack of more detailed information about the flow the term $\overline{uw}/U_0^2$ was neglected, the estimated values of $(\partial W/\partial r)_{r=1}$ agreed reasonably well with the measurements. Some refinements of the theory were attempted by assuming some simple relations for the eddy diffusivity with radial distance which would yield $\overline{vw} = 0$ at $r = 1$, but these attempts were not successful. It appears, therefore, that additional measurements should be made with more refined equipment in order to determine reliably whether or not the analysis presented here can be used to predict velocity profiles in a decaying swirl as well as the average decay characteristics.

The authors are happy to acknowledge the assistance of Mr A. O. Musolf in the experimental part of this study and the financial support of the National Science Foundation.

Appendix. Perturbation solution of the swirl equation

The r-dependent part of the swirl equation is

$$\frac{d^2R_n}{dr^2}+\frac{1}{r}\frac{dR_n}{dr}+\left(\lambda_n^2 U_1-\frac{1}{r^2}\right)R_n=0. \tag{7a}$$

This equation can be solved by a perturbation theory outlined by Courant & Hilbert (1953). Taking the operator L as

$$L=\frac{d^2}{dr^2}+\frac{1}{r}\frac{d}{dr}-\frac{1}{r^2},$$

the unperturbed problem can be written

$$L\bar{R}_n+\bar{\lambda}_n^2\bar{R}_n=0, \tag{A 1}$$

with the boundary conditions $\bar{R}_n(0)=\bar{R}_n(1)=0$. This equation has the solution

$$\bar{R}_n(r)=B_nJ_1(\bar{\lambda}_nr)+D_nY_1(\bar{\lambda}_nr), \tag{A 2}$$

where J_1 is the Bessel function of the first kind of order one, and Y_1 is the Bessel function of the second kind of order one, while B_n and D_n are arbitrary constants. The solution to (A 1) can be found in Wylie (1960).

The boundary conditions imply $D_n=0$ and

$$\bar{\lambda}_1^2=14{\cdot}684,\quad \bar{\lambda}_2^2=49{\cdot}224,\quad \bar{\lambda}_3^2=103{\cdot}490,\quad \bar{\lambda}_4^2=177{\cdot}529....$$

The unperturbed normalized eigenfunctions are then

$$\bar{R}_n(r)=\left(\frac{2}{J_0^2(\bar{\lambda}_n)}\right)^{\frac{1}{2}}J_1(\bar{\lambda}_nr),$$

where J_0 is the Bessel function of the first kind of order zero.

The perturbed differential equation can be written as

$$LR_n-\alpha(1-U_1)\lambda_n^2R_n+\lambda_n^2R_n=0, \tag{A 3}$$

where α is a perturbation parameter. Comparing this equation with (7a) the perturbation parameter is found to be 1·0. This value of α will be used in the final solution. The boundary conditions are $R_n(0)=R_n(1)=0$.

Assuming that the new eigenvalues as well as the new eigenfunctions may be expanded in powers of the perturbation parameter α, then, since the present problem has simple eigenvalues, the solution can be written in the form

$$\left.\begin{aligned} R_n&=\bar{R}_n+\alpha p_n+\alpha^2q_n+\dots\\ \text{and}\quad \lambda_n^2&=\bar{\lambda}_n^2+\alpha\beta_n+\alpha^2\gamma_n+\dots,\end{aligned}\right\} \tag{A 4}$$

where R_n and $\bar{R}_n$ are normalized.

Inserting these relationships into the differential equation (A 3) and equating to zero the coefficients of the various powers of α lead to the following differential equations for the different approximations:

$$\alpha^0\colon\ L\bar{R}_n+\bar{\lambda}_n^2R_n=0, \tag{A 1}$$

$$\alpha^1\colon\ Lp_n+\bar{\lambda}_n^2p_n=(1-U_1)\bar{\lambda}_n^2\bar{R}_n-\beta_n\bar{R}_n, \tag{A 5}$$

$$\alpha^2\colon\ Lq_n+\bar{\lambda}_n^2q_n=(1-U_1)(\bar{\lambda}_n^2p_n+\beta_n\bar{R}_n)-\beta_np_n-\gamma_n\bar{R}_n, \tag{A 6}$$

.....

From these equations the perturbations of various orders can be calculated.

Multiplying (A 5) by $r\bar{R}_m$, since the weight function of J_1 is r, and integrating from $r = 0$ to $r = 1{\cdot}0$ one obtains

$$\int_0^1 r\bar{R}_m L p_n\,dr + \bar{\lambda}_n^2 \int_0^1 r\bar{R}_m p_n\,dr = \int_0^1 \bar{\lambda}_n^2(1-U_1)\,r\bar{R}_n\bar{R}_m\,dr - \beta_n \int_0^1 r\,\bar{R}_n\bar{R}_m\,dr. \quad (A\,7)$$

The first term on the left can be transformed by partial integration and utilization of the relations, $p_n(0) = p_n(1) = 0$ and $L\bar{R}_m = -\bar{\lambda}_m^2\bar{R}_m$, to

$$\int_0^1 r\bar{R}_m L p_n\,dr = -\bar{\lambda}_m^2 \int_0^1 r p_n \bar{R}_m\,dr.$$

Equation (A 7) then becomes

$$a_{nm}(\bar{\lambda}_n^2 - \bar{\lambda}_m^2) = d_{nm} - \beta_n \delta_{nm}, \quad (A\,8)$$

where $$a_{nm} = \int_0^1 r p_n \bar{R}_m\,dr, \quad d_{nm} = \int_0^1 \bar{\lambda}_n^2\,(1-U_1)\,r\bar{R}_n\bar{R}_m\,dr,$$

and $$\delta_{nm} = 0 \quad \text{for} \quad n \neq m \quad \text{and} \quad \delta_{nn} = 1{\cdot}0.$$

By letting $m = n$ one obtains

$$\beta_n = d_{nn}, \quad (A\,9)$$

and taking $m \neq n$

$$a_{nm} = d_{nm}/(\bar{\lambda}_n^2 - \bar{\lambda}_m^2). \quad (A\,10)$$

The quantity a_{nn} is found from the normalization conditions

$$\int_0^1 r R_n^2\,dr = 1 \quad \text{and} \quad \int_0^1 r\bar{R}_n^2\,dr = 1.$$

By expansion of the first condition one finds

$$0 = \alpha \int_0^1 2r\bar{R}_n p_n\,dr + \alpha^2 \int_0^1 r(2\bar{R}_n q_n + p_n^2)\,dr + \ldots.$$

The uniqueness of this power series implies that

$$\int_0^1 2r\bar{R}_n p_n\,dr = \int_0^1 r(2\bar{R}_n q_n + p_n^2)\,dr = \ldots = 0,$$

and therefore $$a_{nn} = 0.$$

If $p_n(r)$ can be expanded in terms of the $\bar{R}_j$, one has

$$p_n(r) = \sum_{j=1}^{\infty}{}' a_{nj}\bar{R}_j = \sum_{j=1}^{\infty}{}' \frac{d_{nj}}{\bar{\lambda}_n - \bar{\lambda}_j}\bar{R}_j,$$

where the sign Σ' denotes summation over the indicated values of j omitting the term for which $j = n$.

Having determined the first approximation, the second approximation

$$q_n(r) = \sum_{m=1}^{\infty} b_{nm}\bar{R}_m$$

is found similarly by using (A 6), from which it follows, as before, that

$$b_{nm}(\bar{\lambda}_n^2 - \bar{\lambda}_m^2) = \sum_{j=1}^{\infty}{}' \frac{\bar{\lambda}_n^2}{\bar{\lambda}_m^2} a_{nj}\,d_{mj} + \frac{\beta_n}{\bar{\lambda}_n^2}\,d_{nm} - \beta_n a_{nm} - \gamma_n \delta_{nm},$$

where $$b_{nm} = \int_0^1 r q_n \bar{R}_m\,dr.$$

Setting $n = m$ one obtains the second perturbation term for the eigenvalues, namely

$$\gamma_n = \sum_{j=1}^{\infty}{}' a_{nj} d_{nj} + \frac{\beta_n^2}{\bar{\lambda}_n^2} = \sum_{j=1}^{\infty}{}' \frac{d_{nj}^2}{\bar{\lambda}_n^2 - \bar{\lambda}_j^2} + \frac{\beta_n^2}{\bar{\lambda}_n^2},$$

while for $n \neq m$ one finds

$$b_{nm} = \frac{1}{\bar{\lambda}_n^2 - \bar{\lambda}_m^2} \left\{ \sum_{j=1}^{\infty}{}' \frac{\bar{\lambda}_n^2}{\bar{\lambda}_m^2} a_{nj} d_{mj} - \frac{\bar{\lambda}_m^2}{\bar{\lambda}_n^2} \beta_n a_{nm} \right\}.$$

To determine b_{nn} one must again employ the normalization condition

$$\int_0^1 r R_n^2 \, dr = 1$$

and set the coefficient of α^2 equal to zero. It follows that

$$b_{nn} = -\frac{1}{2} \int_0^1 r p_n^2 \, dr = -\frac{1}{2} \sum_{j=1}^{\infty}{}' a_{nj}^2,$$

which completely determines the second approximation.

Further approximations may be determined successively in precisely the same manner, but in the present investigation only the first two approximations were used.

The coefficients were evaluated numerically, and they give:

$$R_1 = 3{\cdot}511 J_1(\bar{\lambda}_1 r) + 0{\cdot}116 J_1(\bar{\lambda}_2 r) - 0{\cdot}0165 J_1(\bar{\lambda}_3 r) + \ldots,$$
$$R_2 = -0{\cdot}302 J_1(\bar{\lambda}_1 r) - 4{\cdot}72 J_1(\bar{\lambda}_2 r) + \ldots,$$
$$R_3 = 0{\cdot}072 J_1(\bar{\lambda}_1 r) + 5{\cdot}66 J_1(\bar{\lambda}_3 r) + \ldots,$$
$$R_4 = 6{\cdot}47 J_1(\bar{\lambda}_4 r) + \ldots,$$

and

$$\lambda_1^2 = 14{\cdot}684 + 1{\cdot}757 + 0{\cdot}234 + \ldots \approx 16{\cdot}675,$$
$$\lambda_2^2 = 49{\cdot}224 + 6{\cdot}010 + 0{\cdot}480 + \ldots \approx 55{\cdot}714,$$
$$\lambda_3^2 = 103{\cdot}49 + 12{\cdot}82 + 1{\cdot}55 + \ldots \approx 117{\cdot}86,$$
$$\lambda_4^2 = 177{\cdot}53 + 22{\cdot}50 + 2{\cdot}85 + \ldots \approx 203{\cdot}73.$$

The eigenfunctions can be approximated by

$$R_1 = 3{\cdot}51 J_1(\bar{\lambda}_1 r), \quad R_2 = 4{\cdot}72 J_1(\bar{\lambda}_2 r),$$
$$R_3 = 5{\cdot}66 J_1(\bar{\lambda}_3 r),$$
$$R_4 = 6{\cdot}47 J_1(\bar{\lambda}_4 r).$$

REFERENCES

COURANT, R. & HILBERT, D. 1953 *Methods of Mathematical Physics*, vol. 1. New York: Interscience Publishers Inc.

DEISSLER, R. G. & PERLMUTTER, M. 1960 Analysis of the flow and energy separation in a turbulent vortex flow. *Int. J. Heat & Mass Trans.* **1**, 173.

EINSTEIN, H. S. & Li, H. 1951 Steady vortex flow in a real fluid. *Proc. Heat Transfer & Fluid Mech. Inst.* Palo Alto, Calif.: Stanford University Press.

GAMBILL, W. R., BUNDY, R. D. & WANSBROUGH, R. W. 1961 Heat transfer, burnout, and pressure drop for water in swirl flow through tubes with internal twisted tapes. *Chem. Eng. Symp. Ser.* **5**, 127.

HINZE, J. O. 1959 *Turbulence.* New York: McGraw-Hill Book Co.

JAHNKE, E. & EMDE, F. 1945 *Tables of Functions and Formulae and Curves.* New York: Dover.

KERREBROCK, J. L. & MEGHREBLIAN, R. V. 1961 Vortex containment for the gaseous fission rocket. *J. Aerospace Sci.* **28**, 710.

KEYES, J. J. 1960 An experimental study of gas dynamics in high velocity vortex flow. *Proc. Heat. Trans. & Fluid Mech. Inst.* Palo Alto, Calif.: Stanford University Press.

KREITH, F. & MARGOLIS, D. 1959 Heat transfer and friction in turbulent vortex flow. *Appl. Sci. Res.* A, **8**, 457.

LAUFER, J. 1954 The structure of turbulence in fully developed pipe flow. *NACA Rep.* no. 1174.

MARTINELLI, R. C. 1947 Heat transfer in molten metals. *ASME Trans.* **69**, 947.

MUSOLF, A. O. 1963 An experimental investigation of the decay of a turbulent swirl flow in a pipe. Thesis, University of Colorado.

RAGSDALE, R. G. 1961 NASA research on the hydrodynamics in high velocity vortex flow. *NASA TN D*-288, Sept. 1960. See also *ASME Paper*, no. 61-WA-244.

REYNOLDS, A. J. 1961*a* On the dynamics of turbulent vortical flow. *Z. angew. Math. Phys.* **12**, 149.

REYNOLDS, A. J. 1961*b* Energy flows in a vortex tube. *Z. angew. Math. Phys.* **12**, 343.

SIBULKIN, M. 1962 Unsteady viscous circular flow. Part 3: application to the Ranque–Hilsch vortex tube. *J. Fluid Mech.* **12**, 269.

SMITHBERG, E. & LANDIS, F. 1964 Friction and forced convection heat transfer characteristics in tubes with twisted tape swirl generators. *Trans. ASME, J. Heat Transfer,* **86**, 1.

SONJU, O. K. 1962 A theoretical investigation of the decay of turbulent swirl flow in a Pipe. Thesis, University of Colorado.

TALBOT, L. 1954 Laminar swirling pipe flow. *J. Appl. Mech.* **21**, 1.

WYLIE, C. R. 1960 *Advanced Engineering Mathematics.* New York: McGraw-Hill Book Co.